

Mass Lumping Edge Elements in Three Dimensions

G. Cohen*

P. Monk†

Abstract

The phase accuracy of standard finite difference time domain algorithms in computational electromagnetism limits the type of problem that can be solved. This is because phase error accumulates during the computation and eventually destroys the solution. We propose a new mass-lumped finite element scheme using cubic edge elements which has superior phase accuracy compared to the standard finite difference scheme. The mass lumping is performed carefully to avoid loss of accuracy. We analyze the dispersion error of the mass-lumped cubic scheme and provide a simple numerical example showing the accuracy of the cubic scheme.

Key words: Maxwell's equations, edge elements, mass-lumping.

AMS subject classifications: 65N10, 65N15, 35L50.

1 Introduction

A central problem in computing an approximate solution to a linear hyperbolic problem is the control of phase error accumulation. As a wave propagates through computational space, phase errors accumulate and eventually destroy the accuracy of the solution (see for example [1, 16]). This problem is particularly acute in computational electromagnetism. The desire to compute accurate solutions to electrically large problems (ie. those problems in which a wave must be computed for a large number of cycles) implies the use of vast computational resources. There

*INRIA, Domaine de Voluceau - Rocquencourt, 78153 Le Chesnay, France

†Department of Mathematical Sciences, University of Delaware, Newark DE 19716, USA. Research supported in part by a grant from AFOSR.

ICOSAHOM'95: Proceedings of the Third International Conference on Spectral and High Order Methods. ©1996 Houston Journal of Mathematics, University of Houston.

is an obvious need to find numerical schemes with improved phase accuracy for approximating Maxwell's equations. This paper is devoted to describing a mass-lumped finite element scheme for approximating the Maxwell system in three dimensions. The method is distinguished by having superior phase accuracy properties when compared to the usual finite difference scheme.

In computational electromagnetism, the standard finite difference scheme for approximating the Maxwell system is the Yee scheme [22]. This is a second order accurate (in time and space) staggered grid scheme using leap-frog time stepping. It is very effective for computing the solution of Maxwell's system, but has only second order phase accuracy which limits its applicability to high frequency problems. The cubic finite element method we shall describe has a sixth order accurate phase error (but only fourth order spatial error) and is also a staggered grid scheme (or a mixed method in finite element language).

We are not the first to propose higher order schemes for Maxwell's equations. For example, Tuomela [19] and Petropolis [17] have proposed fourth order finite difference schemes based on extending the Yee approach. This scheme suffers from having a large stencil which complicates the implementation of boundary conditions and the handling of material discontinuities.

A number of authors (for example [21, 20, 15]) have suggested using higher order finite element methods. We follow this approach and will describe a method based on cubic edge finite elements [13] on a mesh of cubes. An important difference in our approach is that we shall show how to mass-lump the scheme using an extension of the approach of [9, 8, 18] while maintaining the accuracy of the scheme. Of course the limitation of using a grid of cubes will need to be relaxed in order to handle curved boundaries. But we will discuss our approach to this problem elsewhere.

One way of fitting curved boundaries is to use tetrahedral elements. However, in the case of edge elements, it is difficult to mass-lump even linear elements [7]. Mass lumping higher order tetrahedral elements is likely to be a challenging problem.

We choose to use the edge elements of Nédélec [13] because these elements have the advantage of allowing control over the divergence of the solution and allow a simple method of satisfying one of the standard electromagnetic boundary conditions. However the price to be paid for this is that the elements are anisotropic and more complex than standard elements. However as we shall discuss here, it is possible to show that the element anisotropy does not adversely effect the phase accuracy of the method. The family we use is cheaper to use (fewer degrees of freedom) than the other edge family of Mur and Nédélec [12, 14].

There are also a number of more innovative approaches for developing phase accurate methods for the Maxwell system. For example Cangellaris [3] has investigated a spectral-cut-off method. At present that method seems limited to periodic problems.

In this paper we shall focus on propagation and phase error properties of the mass-lumped scheme. For this reason we shall only consider a simple cavity problem and ignore such vital aspects of “real” electromagnetic problems as absorbing boundary conditions, complex structures and tensor material properties. These considerations, which are vital for realistic applications, will be discussed in the future.

This work continues our study of two dimensional mass lumped schemes reported in [6, 4]. Here we show show to extend the method to three dimensions, summarize some results about the dispersion behavior of the three dimensional scheme and give the first numerical results in three dimensions.

2 The Maxwell system

As we discussed above, we will limit ourselves to a simple initial boundary value problem for the Maxwell system. Let $\Omega \subset \mathbf{R}^3$ be a domain or cavity filled with a dielectric medium having scalar permittivity ϵ and permeability μ which can be functions of position (even discontinuous functions providing the discontinuities occur at finite element boundaries). The electric field $\mathbf{E} = \mathbf{E}(t, \mathbf{x})$ and magnetic induction $\mathbf{B} = \mathbf{B}(t, \mathbf{x})$ are functions of time t and position \mathbf{x} and satisfy the Maxwell system in Ω :

$$(1) \quad \epsilon \frac{\partial \mathbf{E}}{\partial t} - \nabla \times (\mu^{-1} \mathbf{B}) = -\mathbf{J},$$

$$(2) \quad \frac{\partial \mathbf{B}}{\partial t} + \nabla \times \mathbf{E} = 0.$$

In (1) the function $\mathbf{J} = \mathbf{J}(t, \mathbf{x})$ is a known applied current density. For simplicity we shall assume a simple general-

ized perfectly conducting boundary condition:

$$(3) \quad \mathbf{n} \times \mathbf{E} = \boldsymbol{\gamma} \text{ on the boundary } \Gamma = \partial\Omega.$$

Here $\boldsymbol{\gamma}$ is a known tangential vector field on Γ and \mathbf{n} is the unit outward normal to Γ . Finally, we assume that the initial fields $\mathbf{E}(0, \cdot)$ and $\mathbf{B}(0, \cdot)$ are given. The system (1) and (2) together with the boundary conditions (3) and the initial conditions is a well posed initial boundary value problem for the Maxwell system (at least when Ω is a bounded Lipschitz domain, $\mathbf{J} \in (L^2(\Omega))^3$, and if ϵ and μ are uniformly positive and bounded in $L^\infty(\Omega)$ [10]). We remark that we limit ourselves to dielectric media here since we will focus on wave propagation. A conductivity term can be added without difficulty.

In the special case when $\Omega = \mathbf{R}^3$, $\epsilon = \mu = 1$ and $\mathbf{J} = 0$ the Maxwell system possesses plane wave solutions. The dispersion analysis of (1) and (2) involves describing these solutions. Of course such a dispersion analysis is entirely trivial but we discuss it here for completeness. We suppose that the fields are time harmonic so that

$$\begin{aligned} \mathbf{E}(\mathbf{x}, t) &= \hat{\mathbf{E}}(\mathbf{x}) \exp(-i\omega t) \text{ and} \\ \mathbf{B}(\mathbf{x}, t) &= \hat{\mathbf{B}}(\mathbf{x}) \exp(-i\omega t) \end{aligned}$$

where $\hat{\mathbf{E}}$ and $\hat{\mathbf{B}}$ are vector functions of position and ω is a parameter. Substituting these expressions in (1) and (2) we obtain

$$(4) \quad -i\omega \hat{\mathbf{E}} - \nabla \times \hat{\mathbf{B}} = 0 \quad \text{in } \mathbf{R}^3,$$

$$(5) \quad -i\omega \hat{\mathbf{B}} + \nabla \times \hat{\mathbf{E}} = 0 \quad \text{in } \mathbf{R}^3.$$

Now, if $\omega \neq 0$ we can proceed in the usual way to eliminate the magnetic induction by using (5) in (4) to obtain

$$\omega^2 \hat{\mathbf{E}} + \nabla \times (\nabla \times \hat{\mathbf{E}}) = 0.$$

By standard vector identities this implies that

$$(6) \quad \omega^2 \hat{\mathbf{E}} - \Delta \hat{\mathbf{E}} + \nabla (\nabla \cdot \hat{\mathbf{E}}) = 0.$$

However taking the divergence of (4), and assuming $\omega \neq 0$, we see that $\nabla \cdot \hat{\mathbf{E}} = 0$. Hence (6) becomes

$$(7) \quad \omega^2 \hat{\mathbf{E}} - \Delta \hat{\mathbf{E}} = 0 \quad \text{in } \mathbf{R}^3.$$

Thus each component of $\hat{\mathbf{E}}$ satisfies the standard Helmholtz equation, and the dispersion properties of (4)-(5) are exactly the same as for the wave equation. In particular, we can seek a plane wave solution of (7) of the form

$$\hat{\mathbf{E}} = \hat{\mathbf{E}}_0 \exp(i\mathbf{k} \cdot \mathbf{x})$$

where $\hat{\mathbf{E}}_0$ is a constant vector and $\mathbf{k} = (k_1, k_2, k_3)^T$. For this function to solve (7) it is necessary that ω be related to \mathbf{k} via a *dispersion relation*. There are two possibilities:

$$(8) \quad \text{either } \omega = 0 \text{ or } \omega^2 = k_1^2 + k_2^2 + k_3^2 = |\mathbf{k}|^2.$$

The case $\omega = 0$ corresponds to non-propagating waves, and the case $\omega = \pm|\mathbf{k}|$ corresponds to wave propagation. We shall refer to approximations of the dispersion relation $\omega^2 = |\mathbf{k}|^2$ as the ‘‘physical’’ dispersion relation. Unfortunately, the cubic finite element method in this paper has other non-zero dispersion relations that are termed ‘‘parasitic’’ since they do not have a counterpart in the standard continuous theory. An alternative expression for the dispersion relation corresponding to propagating waves is

$$\omega^2 = \omega_1^2(k_1) + \omega_1^2(k_2) + \omega_1^2(k_3)$$

where $\omega_1^2(k) = k^2$ is the dispersion relation for the one dimensional wave equation. This observation proves useful in analyzing the dispersion properties of the discrete scheme.

3 Edge element discretization

Now let us turn to discretizing (1)-(2) in space. Suppose we construct finite element subspaces as follows (we shall give details of this construction shortly):

$$\begin{aligned} U_h &\subset H(\text{curl}; \Omega) \\ &= \{ \mathbf{u} \in (L^2(\Omega))^3 \mid \nabla \times \mathbf{u} \in (L^2(\Omega))^3 \}, \\ U_{0,h} &\subset H_0(\text{curl}; \Omega) \\ &= \{ \mathbf{u} \in H(\text{curl}; \Omega) \mid \mathbf{n} \times \mathbf{u} = 0 \text{ on } \Gamma \}, \\ V_h &\subset H(\text{div}; \Omega) \\ &= \{ \mathbf{v} \in (L^2(\Omega))^3 \mid \nabla \cdot \mathbf{v} \in L^2(\Omega) \}. \end{aligned}$$

Then the obvious semi-discrete scheme for approximating the Maxwell system is to seek semi-discrete fields $\mathbf{E}_h(t) \in U_h$ and $\mathbf{B}(t) \in V_h$ such that

$$(9) \quad \begin{aligned} (\epsilon \mathbf{E}_{h,t}, \boldsymbol{\phi}) - (\mu^{-1} \mathbf{B}_h, \nabla \times \boldsymbol{\phi}) &= -(\mathbf{J}, \boldsymbol{\phi}), \\ \forall \boldsymbol{\phi} &\in U_{0,h}, \end{aligned}$$

$$(10) \quad \begin{aligned} (\mu^{-1} \mathbf{B}_{h,t}, \boldsymbol{\psi}) - (\mu^{-1} \nabla \times \mathbf{E}_h, \boldsymbol{\psi}) &= 0, \\ \forall \boldsymbol{\psi} &\in V_h, \end{aligned}$$

$$(11) \quad \mathbf{n} \times \mathbf{E}_h = \boldsymbol{\gamma}_h \text{ on } \Gamma,$$

where $(\mathbf{u}, \mathbf{v}) = \int_{\Omega} \mathbf{u} \cdot \mathbf{v} dV$ and $\boldsymbol{\gamma}_h$ is a suitable interpolant of $\boldsymbol{\gamma}$ on Γ . In addition the initial conditions must be enforced (for example by interpolating the initial data). This is an extension of the scheme proposed in [13] to variable ϵ and μ .

The problem with this approach is that the inner product $(\epsilon \mathbf{E}_{h,t}, \boldsymbol{\phi})$ gives rise to a projection matrix which makes it impossible to use a pointwise explicit time stepping scheme to discretize (9)-(10) in time. Following our mass-lumping strategy developed in [4], we mass-lump (9)-(10) by replacing the exact inner products by approximate inner products computed using quadrature. An important difference compared to the two dimensional scheme is that it is now necessary to apply quadrature to all terms in the weak formulation. We define two approximate inner products $(\cdot, \cdot)_{1h}$ and $(\cdot, \cdot)_{2h}$ which approximate (\cdot, \cdot) . Obviously the discrete bilinear forms must be chosen so as to lump the projection matrices for the magnetic and electric equations, preserve accuracy, and result in positive definite diagonal lumped matrices.

Using the approximate inner products, the discrete solutions $(\mathbf{E}_h(t), \mathbf{B}_h(t)) \in U_h \times V_h$ are taken to satisfy

$$(12) \quad \begin{aligned} (\epsilon \mathbf{E}_{h,t}, \boldsymbol{\phi}_h)_{1h} - (\mu^{-1} \mathbf{B}_h, \nabla \times \boldsymbol{\phi}_h)_{2h} &= -(\mathbf{J}, \boldsymbol{\phi}_h)_{1h}, \\ \forall \boldsymbol{\phi}_h &\in U_{0,h}, \end{aligned}$$

$$(13) \quad \begin{aligned} (\mu^{-1} \mathbf{B}_{h,t}, \boldsymbol{\psi}_h)_{2h} + (\mu^{-1} \nabla \times \mathbf{E}_h, \boldsymbol{\psi}_h)_{2h} &= 0, \\ \forall \boldsymbol{\psi}_h &\in V_h, \end{aligned}$$

together with the boundary condition (11). In each case, for $i = 1$ or 2 the quadrature has the form

$$(14) \quad (\mathbf{u}, \mathbf{v})_{ih} = (u_1, v_1)_{1ih} + (u_2, v_2)_{2ih} + (u_3, v_3)_{3ih},$$

where the quadratures used to compute each term use quadrature points at the interpolation points for the corresponding component of the solution.

It remains to describe the quadratures and the spaces U_h , $U_{0,h}$ and V_h . We suppose that Ω has been covered by a mesh consisting of translates of the ‘‘unit cell’’ $[0, h]^3$. Obviously this greatly restricts the class of domains Ω . We could allow parallel-piped boxes, but the extension of the scheme to isoparametric hexahedra is much more complex and will be addressed in another paper.

On each cube in the mesh, the electric and magnetic fields are represented by polynomials. In order to define these polynomials, we need to introduce some notation which we do next. Let $-1 = \hat{x}_1^L < \hat{x}_2^L < \hat{x}_3^L < \hat{x}_4^L = 1$ be the cubic Gauss-Lobatto quadrature points in $[-1, 1]$ with corresponding quadrature weights \hat{w}_1^L , \hat{w}_2^L , \hat{w}_3^L and \hat{w}_4^L . Note that $\hat{w}_1^L = \hat{w}_4^L$. By mapping $[-1, 1]$ onto $[0, h]$ using an affine map, we obtain the Gauss-Lobatto points $0 = x_1^L < x_2^L < x_3^L < x_4^L = h$ on $[0, h]$ with associated weights $w_i^L = \hat{w}_i^L h/2$, $1 \leq i \leq 4$. Then we define the basis polynomials $\{l_i(x)\}_{i=1}^4$ of degree 3 by requiring that $l_i(x_j^L) = \delta_{ij}$, $1 \leq j \leq 4$. Thus $\{l_i(x)\}_{i=1}^4$ are the Lagrange basis functions associated with the Gauss-Lobatto points.

In the same way, let $x_1^G < x_2^G < x_3^G$ be the quadratic Gauss points in $[0, h]$ (obtained by mapping the Gauss points in $[-1, 1]$ to $[0, h]$) with associated quadrature weights $\{w_i^G\}_{i=1}^3$. We define the quadratic Lagrange basis polynomials $\{g_i(x)\}_{i=1}^3$ by $g_i(x_j^G) = \delta_{ij}$, $1 \leq j \leq 3$. Having defined these polynomials we can define the cubic edge elements used in this paper. These were proposed and analyzed in [13]. On the element $[0, h]^3$, the discrete approximation $\mathbf{E}_h = (E_{1h}, E_{2h}, E_{3h})$ of \mathbf{E} is represented as follows

$$(15) \quad E_{1h}(x, y, z) = \sum_{i=1}^3 \sum_{j=1}^4 \sum_{k=1}^4 E_{ijk}^{(1)} g_i(x) l_j(y) l_k(z),$$

$$(16) \quad E_{2h}(x, y, z) = \sum_{i=1}^4 \sum_{j=1}^3 \sum_{k=1}^4 E_{ijk}^{(2)} l_i(x) g_j(y) l_k(z),$$

$$(17) \quad E_{3h}(x, y, z) = \sum_{i=1}^4 \sum_{j=1}^4 \sum_{k=1}^3 E_{ijk}^{(3)} l_i(x) l_j(y) g_k(z),$$

where $\{E_{ijk}^{(1)}, E_{ijk}^{(2)}, E_{ijk}^{(3)}\}$ are the degrees of freedom of the solution. The finite element solution on other elements is represented by translations of the basis functions used above (with different coefficients!).

To obtain a globally curl conforming element, E_{1h} is chosen to be continuous in across faces in the mesh that are normal to the y and z axes, but in general, it is discontinuous faces in the mesh that are normal to the x axis. Similarly E_{2h} is continuous across faces normal to the x and z axes and E_{3h} is continuous across faces normal to the x and y axes. The space U_h can then be assembled in the usual finite element way. The space $U_{h,0}$ is the subspace of U_h consisting of those functions with a vanishing tangential component on Γ . This can be found simply by setting the degrees of freedom associated with edges or faces on Γ to zero.

On $[0, h]^3$, the discrete magnetic induction $\mathbf{B}_h = (B_{1h}, B_{2h}, B_{3h})^T$ is represented by

$$(18) \quad B_{1h}(x, y, z) = \sum_{i=1}^4 \sum_{j=1}^3 \sum_{k=1}^3 B_{ijk}^{(1)} l_i(x) g_j(y) g_k(z),$$

$$(19) \quad B_{2h}(x, y, z) = \sum_{i=1}^3 \sum_{j=1}^4 \sum_{k=1}^3 B_{ijk}^{(2)} g_i(x) l_j(y) g_k(z),$$

$$(20) \quad B_{3h}(x, y, z) = \sum_{i=1}^3 \sum_{j=1}^3 \sum_{k=1}^4 B_{ijk}^{(3)} g_i(x) g_j(y) l_k(z),$$

where $\{B_{ijk}^{(1)}, B_{ijk}^{(2)}, B_{ijk}^{(3)}\}$ are the degrees of freedom of the solution.

To obtain a globally divergence conforming element, B_{1h} is continuous across faces in the mesh that are normal to the x axis, but in general discontinuous across other faces. Similarly B_{2h} is continuous across faces normal to the y axis and B_{3h} is continuous across faces normal to the z axis. The space V_h can then be assembled in the usual finite element way.

Figure 1 shows the distribution of degrees of freedom for the first component of the electric and magnetic fields. Note that the polynomials used to represent \mathbf{E}_h and \mathbf{B}_h are of different degrees in different directions, and different for each component so it is not clear how the discrete dispersion relation will behave.

The quadratures used to compute $(\cdot, \cdot)_{1h}$ and $(\cdot, \cdot)_{2h}$ use quadrature points at the interpolation points for the corresponding component of the solution. Thus, we approximate

$$(21) \quad \int_{[0,h]^3} u_1 v_1 dV \approx \sum_{i=1}^3 \sum_{j=1}^4 \sum_{k=1}^4 u_1(x_i^G, x_j^L, x_k^L) v_1(x_i^G, x_j^L, x_k^L) \cdot \omega_i^G \omega_j^L \omega_k^L.$$

and $(u_1, v_1)_{1ih}$ (see (14)) is obtained by adding quadratures of the type (21) over all elements. The remaining quadratures are defined similarly. Using these quadratures and the fact that the basis functions are Lagrange interpolants at the quadrature points results in a diagonal matrix multiplying each time derivative term when the discrete equations are written in matrix form. The fact that Gauss or Gauss-Lobatto quadrature is used in each direction implies that the accuracy of the finite element scheme is not spoiled.

4 Dispersion analysis

Taking $\Omega = \mathbf{R}^3$, $\epsilon = \mu = 1$ and $\mathbf{J} = 0$ in (12) and (13) we can perform a discrete dispersion analysis on the finite element scheme outlined above. We start the dispersion analysis of the discrete scheme by seeking discrete solutions of the form

$$\begin{aligned} \mathbf{E}_h(\mathbf{x}, t) &= \hat{\mathbf{E}}_h(\mathbf{x}) \exp(-i\omega t), \text{ and} \\ \mathbf{B}_h(\mathbf{x}, t) &= \hat{\mathbf{B}}_h(\mathbf{x}) \exp(-i\omega t) \end{aligned}$$

where $\hat{\mathbf{E}}_h \in U_h$ and $\hat{\mathbf{B}}_h \in V_h$. Then (12)-(13) becomes

$$(22) \quad -i\omega(\hat{\mathbf{E}}_h, \boldsymbol{\psi}_h)_{1h} - (\hat{\mathbf{B}}_h, \nabla \times \boldsymbol{\psi}_h)_{2h} = 0 \quad \forall \boldsymbol{\psi}_h \in U_h,$$

$$(23) \quad -i\omega(\hat{\mathbf{B}}_h, \boldsymbol{\phi}_h)_{2h} - (\nabla \times \hat{\mathbf{E}}_h, \boldsymbol{\phi}_h)_{2h} = 0 \quad \forall \boldsymbol{\phi}_h \in V_h,$$

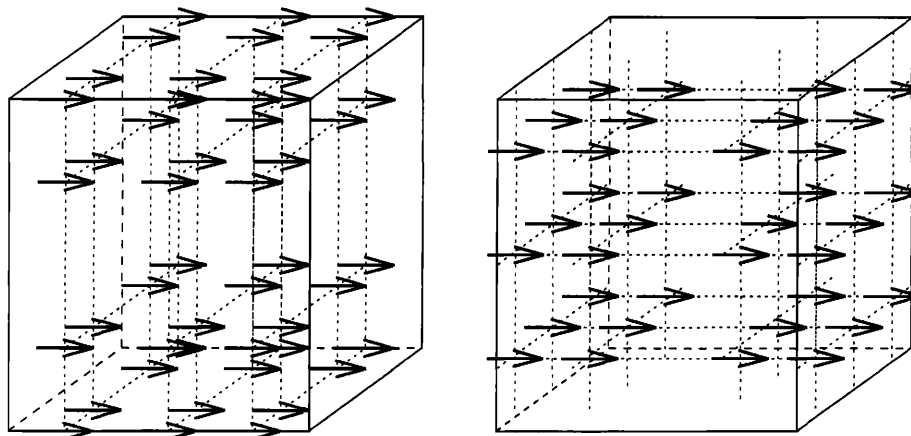


Figure 1: Here we show the distribution of degrees of freedom for the first component of the electric and magnetic fields on an element (electric field - left, magnetic induction - right). The degrees are located at Gauss or Gauss-Lobatto points in each coordinate and are show by the bold face arrows. There are some electric degrees associated with edges of the grid and this is the origin of the name “edge elements” for the electric field. For the magnetic field the degrees of freedom are either internal to an element or associated with faces.

we cannot find finite element functions $\hat{\mathbf{E}}_h$ and $\hat{\mathbf{B}}_h$ that behave like $\exp(i\mathbf{k} \cdot \mathbf{x})$ in space since $\hat{\mathbf{E}}_h$ and $\hat{\mathbf{B}}_h$ are piecewise polynomials. Instead we demand that $\hat{\mathbf{E}}_h$ and $\hat{\mathbf{B}}_h$ behave like $\exp(i\mathbf{k} \cdot \mathbf{x})$ on the level of the mesh, so that if \mathbf{e}_i is the i th unit vector

$$(24) \quad \begin{aligned} & \hat{\mathbf{E}}_h(\mathbf{x} + l h \mathbf{e}_1 + m h \mathbf{e}_2 + n h \mathbf{e}_3) = \\ & \hat{\mathbf{E}}_h(\mathbf{x}) \exp(i(l h k_1 + m h k_2 + n h k_3)) \end{aligned}$$

and similarly for $\hat{\mathbf{B}}_h$. In particular let us consider the the first component of $\hat{\mathbf{E}}_h$ denoted \hat{E}_{h1} . This function is discontinuous as a function of x across faces in the mesh normal to the x axis, but it is continuous as a function of y or z across the remaining faces. Thus we are only concerned with (24) in the y and z directions:

$$\hat{E}_{h1}(\mathbf{x} + l h \mathbf{E}_2 + m h \mathbf{E}_3) = \hat{E}_{h1}(\mathbf{x}) \exp(i k_2 h l) \exp(i k_3 h m).$$

This equation relates \hat{E}_{h1} on faces normal of $[0, h]^3$ to the y or z axis to the value on the opposite face. Motivated by this we define the 4×3 matrix P_x by

$$P_x = \left(\begin{array}{c} I \\ \exp(i k_1 h), 0, 0 \end{array} \right)$$

where I is the 3×3 identity matrix. The matrices P_y and P_z are defined similarly with k_1 replaced by k_2 and k_3 respectively.

We shall also need the following notation. Let M^G be the 3×3 diagonal matrix with $(\omega_1^G, \dots, \omega_3^G)$ on the main

diagonal and let M^L be the 4×4 diagonal matrix with $(\omega_1^L, \dots, \omega_4^L)$ on the main diagonal. We also define $D^{(1)}$ to be the 4×3 matrix with $D_{ij}^{(1)} = \int_0^h l'_i(x) g_j(x) dx$. Finally let I_G be the 3×3 identity matrix and I_L be 4×4 identity matrix.

The following theorem holds [5]:

Theorem 4.1 *Let $0 \leq k_i h \leq \pi$, $1 \leq i \leq 3$ and suppose $\omega_h \neq 0$ where ω_h is the dispersion relation for the first kind edge elements with mass-lumping. Then*

$$\omega_h^2(\mathbf{k}) = \omega_{1h}^2(k_1) + \omega_{2h}^2(k_2) + \omega_{3h}^2(k_3)$$

where ω_{1h}^2 is an eigenvalue for

$$(25) \quad P_x^* D^{(1)} M_G^{-1} D^{(1)T} P_x \mathbf{u}_1 - \omega_{1h}^2 P_x^* M_L P_x \mathbf{u}_1 = 0$$

and similarly for ω_{2h} and ω_{3h} (with x replaced by y and z).

Remarks.

1. The proof of this theorem follows the same outline as derivation of the the dispersion relations for the continuous problem given in the introduction.
2. Equation (25) is exactly the equation arising from a dispersion analysis of the one dimensional wave equation discretized using finite elements and mass-lumped by Gauss–Lobatto point integration [4]. Thus dispersion relations are available [18].

3. Despite the use of anisotropic basis functions (different degrees in different directions), from the point of view of phase error the method behaves as if full cubic polynomials have been used in all directions.
4. If we do not mass lump (so use (9)-(10) rather than (12)-(13)) the same conclusion holds if we replace M_G and M_L by suitable non-diagonal inner product matrices for the appropriate elements.

From [18] we know that (25) has three dispersion relations (we have suppressed the dependency on x):

$$(26) \quad \omega_h^2(k) = \lambda_h^1(k) \approx k^2 \left(1 - \frac{h^6 k^6}{302400} + O(h^8 k^8) \right),$$

$$(27) \quad \omega_h^2(k) = \lambda_h^2(k) \approx k^2 \left(\frac{30}{h^2 k^2} + O(1) \right),$$

$$(28) \quad \omega_h^2(k) = \lambda_h^3(k) \approx k^2 \left(\frac{60}{h^2 k^2} + O(1) \right).$$

The first dispersion relation (26) is the “physical” dispersion relationship corresponding to a sixth order approximation to the true dispersion relation $\omega^2 = k^2$ for the one dimensional wave equation. The remaining dispersion relations (27) and (28) are parasitic modes. These modes do not seem to cause catastrophic problems in practice, but must be taken into account when determining the stability of the scheme.

Using (26)-(28) we have the following corollary:

Corollary 4.1 *There are 27 non zero dispersion relations for the cubic edge finite element scheme described here. They are*

$$\omega_{h,i,j,k}^2(\mathbf{k}) = \lambda_h^i(k_1) + \lambda_h^j(k_2) + \lambda_h^k(k_3),$$

for $1 \leq i, j, k \leq 3$. One mode, $\omega_{h,1,1,1}^2(\mathbf{k})$, is a sixth order approximation to the physical mode given in (8). The remaining 26 modes are parasitic.

One more point is that using this corollary and the results of [18] we can show that

$$(29) \quad \max_{1 \leq i,j,k \leq 3} \max_{hk} h^2 \omega_{h,i,j,k}^2(\mathbf{k}) = 18(6 + \sqrt{29}).$$

This result will allow us to give a stability condition for the fully discrete scheme.

5 Time stepping

For a practical implementation of (12)-(13) it is necessary to discretize in time. In [4], we have shown that in two dimensions it is best to use a fourth order leap-frog time stepping scheme when cubic finite elements are used in space.

An obvious question is whether this conclusion holds in three dimensions.

We shall start by presenting a second order in time scheme. If we number the degrees of freedom for \mathbf{E}_h and \mathbf{B}_h we can write the unknowns as vectors \vec{E}_h and \vec{B}_h , then (12)-(13) may be written as the following matrix ordinary differential equation:

$$(30) \quad M_E \frac{d\vec{E}_h}{dt} - C^T \vec{B}_h = M_E \vec{J},$$

$$(31) \quad M_B \frac{d\vec{B}_h}{dt} + C \vec{E}_h = 0,$$

where (30) applies to the internal degrees of freedom of \mathbf{E}_h and the boundary degrees are determined by (11). The most important feature of these equations is that M_E and M_B are diagonal matrices which is a direct result of our lumping strategy. The matrix C corresponds to a discrete curl, and the vector \vec{J} is determined from the given function \mathbf{J} .

To obtain a second order time stepping scheme, we use a leap-frog scheme (as is standard for finite difference methods [22]). We let $\vec{E}_h^n \approx \vec{E}_h(n\Delta t)$ and $\vec{B}_h^{n+1/2} \approx \vec{B}_h((n + 1/2)\Delta t)$ where Δt is the time step. Then the fully discrete electric and magnetic fields are determined by solving successively

$$M_E \left(\frac{\vec{E}_h^{n+1} - \vec{E}_h^n}{\Delta t} \right) - C^T \vec{B}_h^{n+1/2} = M_E \vec{J}^{n+1/2},$$

$$M_B \left(\frac{\vec{B}_h^{n+3/2} - \vec{B}_h^{n+1/2}}{\Delta t} \right) + C \vec{E}_h^{n+1} = 0.$$

These equations may be solved rapidly since M_E and M_B are diagonal.

If $\Omega = \mathbf{R}^3$, we can use the dispersion analysis to show that the time stepping scheme is stable provided the following Courant condition is satisfied:

$$\frac{\Delta t}{h} \leq \frac{2}{\sqrt{18(7 + \sqrt{29})}} \approx 0.13.$$

where we have used (29).

This time stepping scheme is called a “2-4” scheme since it is formally second order in time and the use of cubic elements in space is expected to provide fourth order accuracy in space. The fourth order accuracy in space is a known superconvergence result if the method is not mass lumped [11], but has not yet been proved for the mass lumped case.

To construct a fourth order in time scheme, we adopt the modified equation approach which corrects the error

in the leap-frog scheme. The scheme is derived in [4] and can be summarized as follows: if we define

$$\mathcal{A} = M_E^{-1} C^T \text{ and } \mathcal{B} = -M_B^{-1} C$$

then at interior points

$$\begin{aligned} \vec{E}_t^{n+1/2} &= \mathcal{A} \vec{B}^{n+1/2} + \vec{J}^{n+1/2} \\ \vec{E}_{tt}^{n+1/2} &= \mathcal{A} \mathcal{B} \left(\mathcal{A} \vec{B}^{n+1/2} + \vec{J}^{n+1/2} \right) + \vec{J}_{tt}^{n+1/2}, \end{aligned}$$

while at boundary points $\vec{E}_t^{n+1/2}$ and $\vec{E}_{tt}^{n+1/2}$ are given by time derivatives of γ .

Using these equalities in a Taylor expansion of $\vec{E}^{n+1} - \vec{E}^n$ about $t = (n + 1/2)\Delta t$ and discarding higher order terms gives us the following time stepping scheme for the electric field

$$(32) \quad \vec{E}^{n+1} = \vec{E}^n + \Delta t \vec{E}_t^{n+1/2} + \frac{(\Delta t)^3}{24} \vec{E}_{tt}^{n+1/2}.$$

This is a corrected leap-frog scheme.

The time stepping scheme for the magnetic induction is obtained in the same way using the magnetic analogue of (32). Using this time stepping scheme, we have a locally fourth order accuracy in time. The scheme is termed a ‘4-4’ scheme since it is formally 4th order in time and expected to be 4th order in space. The stability constraint can be shown (again using the bound (29)) to be

$$\Delta t \leq 0.381h.$$

This is almost three times the stability limit for the 2-4 scheme (but the work per time step is approximately three times the work for a single 2-4 time step). Thus the fourth order in time accuracy is gained at almost no extra cost compared to the 2-4 scheme.

To demonstrate the improvement in phase velocity of the fully discrete 4-4 scheme compared to the Yee scheme we show a graph of phase velocity defined by $\omega_h/|\mathbf{k}|$ against the reciprocal of the number of grid points per wavelength in Figure 2 for waves traveling along the x axis (ie $\mathbf{k} = (k_1, 0, 0)$). For the Yee scheme, we choose $\Delta t/h = 1/\sqrt{3}$, and for the 4-4 scheme we choose $\Delta t/h = 0.3$. The exact phase velocity is unity regardless of \mathbf{k} , and both the Yee scheme and the cubic 4-4 scheme underestimate this phase velocity. However the cubic 4-4 scheme is much closer to the ideal.

6 Numerical results

In order to compare the cubic method to the standard Yee finite difference scheme we have performed a simple

computational comparison of the methods. We take $\Omega = [0, 2]^3$ and mesh Ω by subdividing into $N \times N \times N$ cubes.

For the Yee scheme the time step is chosen to be the optimal step (the maximum step consistent with stability). For the 2-4 cubic scheme, we choose either

$$\begin{aligned} \Delta t &\approx \frac{0.2h}{\sqrt{3}} \text{ (this is approximately} \\ &\quad \text{the Courant stability limit),} \\ \text{or } \Delta t &\approx \min\left(\frac{0.2h}{\sqrt{3}}, \frac{h^2}{3}\right) \end{aligned}$$

and for the cubic 4-4 scheme we use $\Delta t \approx 0.3h$.

The exact solution is a Gaussian wave given by

$$\mathbf{E} = \mathbf{E}_0 g(\mathbf{k} \cdot \mathbf{x} - t) \quad \text{and } \mathbf{B} = \mathbf{B}_0 g(\mathbf{k} \cdot \mathbf{x} - t)$$

where

$$\mathbf{k} = (\cos(\theta) \cos(\phi), \sin(\theta), \cos(\theta) \sin(\phi))$$

and $\theta = \phi = 0.5$. Also

$$\begin{aligned} \mathbf{E}_0 &= (-\sin(\theta) \cos(\phi), \cos(\theta), -\sin(\theta) \sin(\phi)) \\ \mathbf{B}_0 &= (-\sin(\phi), 0, \cos(\phi)), \end{aligned}$$

Finally the function $g(t)$ is given by

$$g(t) = \begin{cases} \frac{\exp(-10(s-1)^2) - \exp(-10)}{1 - \exp(-10)} & 0 \leq t \leq 2 \\ 0 & \text{otherwise.} \end{cases}$$

The boundary data γ is computed from the exact solution and $\mathbf{J} = 0$. The solution is not aligned with a particular mesh direction.

To obtain a quantitative comparison of the error in the various schemes, we shall display plots of the discrete relative L^2 error as a function of the number of degrees of freedom in the problem (number of unknowns). The discrete L^2 error is defined as follows. Let π_h^E and π_h^B be the interpolation operators for the electric and magnetic field spaces (obviously these operators are different for the cubic and Yee schemes). Then the relative discrete L_2 error is defined to be

$$(33) \quad \frac{(\|\pi_h^E \mathbf{E}(t) - \mathbf{E}_h(t)\|^2 + \|\pi_h^B \mathbf{B}(t) - \mathbf{B}_h(t)\|^2)^{1/2}}{(\|\pi_h^E \mathbf{E}(t)\|^2 + \|\pi_h^B \mathbf{B}(t)\|^2)^{1/2}}$$

(recall $\epsilon = \mu = 1$) and we evaluate this error at $t = 3$.

When we use $\Delta t = O(h)$ in the cubic 2-4 scheme, the error is almost entirely due to time stepping error (since this is second order rather than fourth order for the spatial error). The overall convergence rate is second order

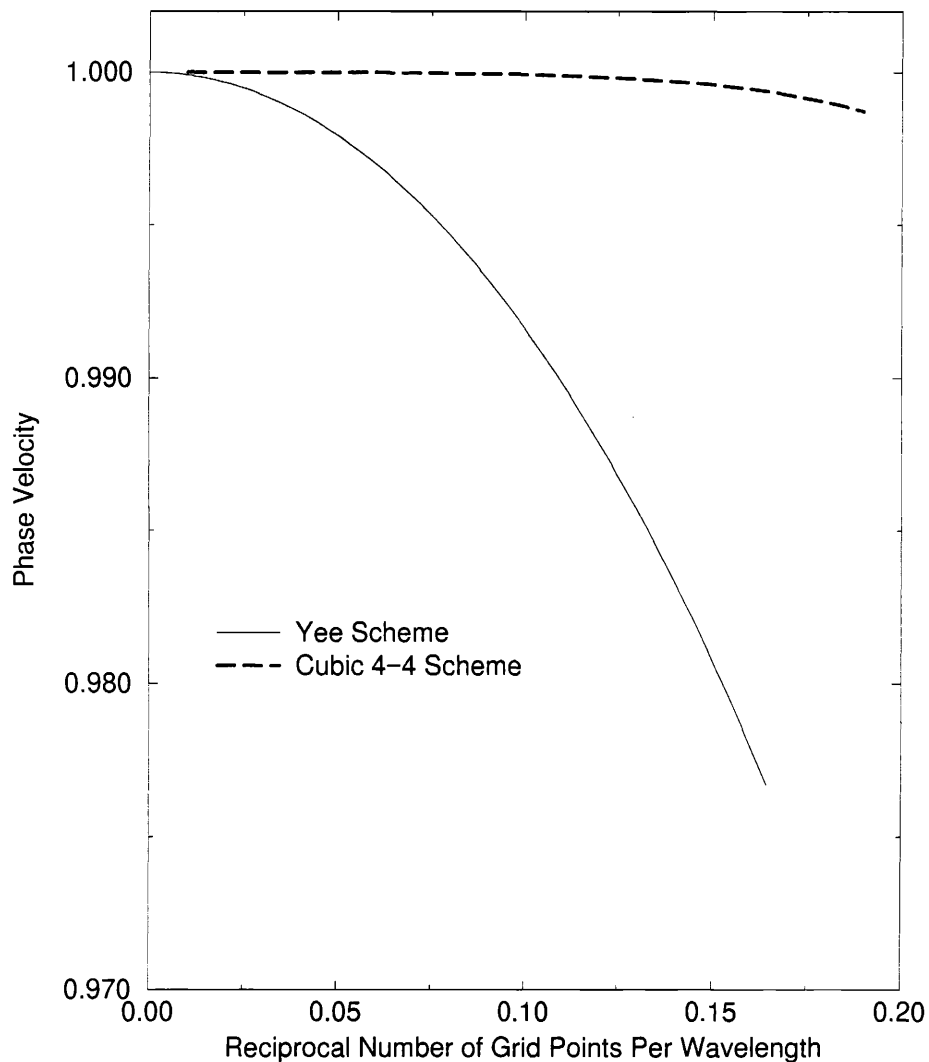


Figure 2: Here we show a graph of the discrete phase velocity (defined by $\omega_h/|k|$) against the reciprocal number of grid points per wavelength for waves traveling along the x axis. In the case of the Yee scheme, we choose $\Delta t/h = 1/\sqrt{3}$ which is optimal. For the 4-4 scheme we show the phase velocity for $\Delta t/h = 0.3$. These choices of Courant condition are the same as those used for the numerical experiments in Section 6. Ideally the phase velocity should be constant and equal to one independent of the number of grid points per wavelength.

and the results in Figure 3 show that the method has approximately the same error (for a given total number of degrees of freedom) as the Yee scheme. If however we use $\Delta t = O(h^2)$ in the 2-4 scheme, the error in the discrete scheme is now $O(h^4)$ and for a given number of degrees of freedom the cubic scheme is more accurate than the Yee scheme (provided h is small enough). This choice is not practical in general since it results in a very small time step.

For the 4-4 scheme, the choice of $\Delta t = O(h)$ results in a scheme with error $O(h^4)$ and with a reasonable time step size. Again the results are shown in Figure 3.

7 Conclusion

We have described a cubic mass-lumped edge finite element scheme for approximating the Maxwell system and have derived the dispersion relations for the semi-discrete scheme. These show a sixth order accurate dispersion relation (although the scheme is only expected to be fourth order accurate in amplitude due to the use of cubic basis functions). We then showed how to discretize the method in time using either a second order or fourth order leapfrog scheme and derived the stability bound for these schemes.

Numerical results (for propagating a Gaussian pulse a short distance) show that the cubic method can be more accurate than the Yee scheme provided a sufficiently accurate time stepping scheme is used. The results also suggest that the fourth order in time offers substantial advantages over the second order in time scheme.

To be truly useful the scheme must be developed further. In particular we need to show how to deal with curved boundaries and how to implement an absorbing condition to terminate infinite domain calculations. The problem of curved boundaries is the most difficult since it appears likely that the use of Berenger's perfectly matched absorbing layer [2] will be possible with our cubic scheme and that this will result in a good absorbing condition. We are currently investigating mapping schemes to fit curved boundaries and hope to report on a complete method soon.

References

- [1] A. Bayliss, C.I. Goldstein, and E. Turkel. On accuracy conditions for the numerical computation of waves. *J. Comp. Phys.*, 59:396–494, 1985.
- [2] J.P. Berenger. A Perfectly Matched Layer for the Absorption of Electromagnetics Waves. *J. Comput. Phys.*, 114:185–200, 1994.
- [3] A.C. Cangellaris, M. Gribbons, and G. Sohos. A hybrid spectral/FDTD method for the electromagnetic analysis of guided waves in periodic structures. *IEEE Microwave and Guided Wave Letters*, 3:375–377, 1993.
- [4] G. Cohen and P. Monk. Gauss point mass lumping schemes for Maxwell's equations: I Two dimensions. submitted for publication.
- [5] G. Cohen and P. Monk. Gauss point mass lumping schemes for Maxwell's equations: II Three dimensions. submitted for publication.
- [6] G. Cohen and P. Monk. Gauss point mass lumping schemes in electromagnetism. *COMPEL*, 13 A:293–298, 1994.
- [7] Y. Haugazeau and P. Lacoste. Condensation de la matrice masse pour les éléments finis mixtes de $h(\text{rot})$. *Comptes Rendu, Series 1*, 316:509–512, 1993.
- [8] J-P. Hennart. Topics in finite element discretization of parabolic evolution problems. *Lecture Notes in Mathematics*, 909:185–199, 1982.
- [9] J-P. Hennart, E. Sainz, and M. Villegas. On the efficient use of the finite element method in static neutron diffusion calculations. *Computational Methods in Nuclear Engineering*, 1:3–87, 1979.
- [10] R. Leis. *Initial Boundary Value Problems in Mathematical Physics*. John Wiley, New York, 1988.
- [11] P. Monk. Superconvergence of finite element approximations to Maxwell's equations. *Numerical Methods for Partial Differential Equations*, 10:793–812, 1994.
- [12] G. Mur and A.T. de Hoop. A finite-element method for computing three-dimensional electromagnetic fields in inhomogeneous media. *IEEE Trans. Magnetics*, MAG-21:2188–2191, 1985.
- [13] J.C. Nédélec. Mixed finite elements in \mathbf{R}^3 . *Numer. Math.*, 35:315–341, 1980.
- [14] J.C. Nédélec. A new family of mixed finite elements in \mathbf{R}^3 . *Numer. Math.*, 50:57–81, 1986.
- [15] A. F. Peterson. Vector finite element formulation for scattering from two-dimensional heterogeneous bodies. *IEEE Antennas and Propagation*, 43:357–365, 1994.

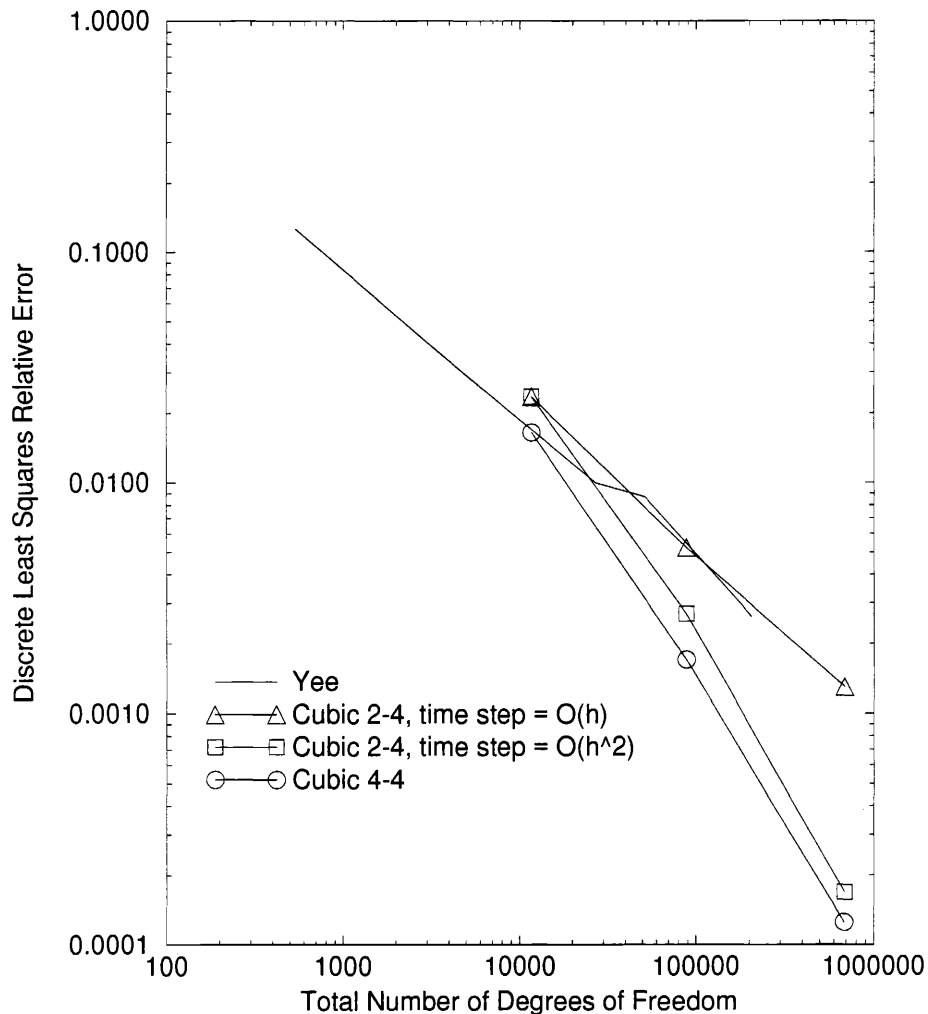


Figure 3: Here we show the discrete L^2 error defined by (33) against the total number of degrees of freedom for the Yee scheme, the cubic 2-4 scheme and the cubic 4-4 scheme. This error includes both phase and amplitude error. The Yee scheme and cubic 2-4 scheme with $\Delta t = O(h)$ converge with error $O(h^2)$ and there is not an obvious advantage to the cubic scheme since the error is close to the Yee scheme for a given number of unknowns. If a more accurate time stepping scheme is used (cubic 2-4 scheme with $\Delta t = O(h^2)$ or the cubic 4-4 scheme) the cubic scheme now converges at the expected rate of $O(h^4)$ and rapidly becomes more accurate than the Yee scheme. These results suggest that the cubic 4-4 scheme is to be preferred to the cubic 2-4 scheme.

- [16] A.F. Peterson and R.J. Baca. Error in the finite element discretization of the scalar Helmholtz equation over electrically large regions. *IEEE Microwave and Guided Wave Letters*, 1:219–221, 1991.
- [17] P.G. Petropoulos. Phase error analysis control for FD-TD methods of second and fourth order accuracy. *IEEE Trans. Antennas Propagat.*, 42:859–862, 1994.
- [18] N. Tordjman. *Elements finis d'ordre élevé avec condensation de masse pour l'équations des ondes*. PhD thesis, Université Paris IX Dauphine, 1995.
- [19] J. Tuomela. Fourth-order schemes for the wave equation, Maxwell equations, and linearized elastodynamic equations. *Numerical Methods for Partial Differential Equations*, 10:33–64, 1994.
- [20] J.S. Wang and N. Ida. Curvilinear and higher order 'edge' finite elements in electromagnetic field computation. *IEEE Trans. on Magnetism*, 29:1491–1493, 1993.
- [21] J.P. Webb and B. Forghani. Hierarchical scalar and vector tetrahedra. *IEEE Trans. on Magnetism*, 29:1495–1498, 1993.
- [22] K.S. Yee. Numerical solution of initial boundary value problems involving Maxwell's equations in isotropic media. *IEEE Trans. on Antennas and Propagation*, AP-16:302–307, 1966.

